

Krylov complexity of many-body localization: Operator localization in Krylov basis

Fabian Ballar Trigueros¹ and Cheng-Ju Lin¹

¹*Perimeter Institute for Theoretical Physics, Waterloo, Ontario, Canada N2L 2Y5*

Motivated by the recent developments of quantum many-body chaos, characterizing how an operator grows and its complexity in the Heisenberg picture has attracted a lot of attentions. In this work, we study the operator growth problem in a many-body localization (MBL) system from a recently proposed Lanczos algorithm perspective. Using the Krylov basis, the operator growth problem can be viewed as a single particle hopping problem on a semi-infinite chain with the hopping amplitudes given by the Lanczos coefficients. We find that, in the MBL phase, the Lanczos coefficients scales $\sim n/\ln(n)$ asymptotically, same as in the ergodic phase, but with an additional even-odd alteration and effective randomness. Extrapolating the Lanczos coefficients to the thermodynamic limit, we study the spectral function and also find that the corresponding single-particle problem is localized for both unextrapolated and extrapolated Lanczos coefficients, resulting in a bounded “Krylov complexity” in time. For the MBL phenomenological model, the Lanczos coefficients also have an even-odd alteration, but approaching to constants asymptotically. We also find that the Krylov complexity grows linearly in time for the MBL phenomenological model.

I. INTRODUCTION

Motivated by the recent developments of quantum many-body chaos, characterizing how a operator grows and its complexity under an unitary many-body dynamics in the Heisenberg picture has been a research focus across different subfields of physics [1–6]. A popular characterization of the growth of an operator is by the out-of-time-ordered commutators (correlators), which emphasizes the operator growth in the space-time picture [7–17]. Another characterization is via the operator entanglement, which has also been studied in various systems [18–24].

Recently, Parker *et al.* [25] proposes a different characterization of operator growth from the perspective of recursive method (or Lanczos algorithm). The Lanczos algorithm generates a set of so-called Krylov basis which is used to represent the operator, and the dynamics is therefore encoded in the time-dependent coefficients of the basis. In a sense which we will make precise later, the operator growth problem in this basis can be viewed as the evolution of a single particle wavefunction, hopping on a semi-infinite chain with the hopping amplitudes given by the Lanczos coefficients generated by the Lanczos algorithm, initialized on the first site. One can therefore define various complexity measures from this point of view. For example, Ref. [25] defines the Krylov complexity to be the mean position the corresponding single particle. Ref. [26] also proposes Krylov entropy, which measures the degree of spreading of the corresponding single particle wavefunction on the semi-infinite chain.

Ref. [25] hypothesizes that, for a chaotic system, the Lanczos coefficients grow as fast as possible asymptotically. For a local Hamiltonian, the Lanczos coefficients are upper bounded by a function linearly in the Krylov order asymptotically (with a logarithmic correction in 1D), which implies that the Krylov complexity grows exponentially in time (or grows as a stretched exponential in time in 1D). In contrast, in the integrable models, the Lanczos coefficients grow as a square root of the Krylov

order or as a constant [25, 27]. Krylov complexity was also studied with some general considerations [28, 29] and studied in conformal field theories [30], in models with holographic correspondence [26] and in models with strong and almost strong edge modes [31, 32].

In this paper, we study the operator growth and the Krylov complexity in a many-body localized (MBL) system [33–36] to contrast and complement with the previous results in the chaotic and integrable models. Operator growth in MBL systems have been studied using the characterization of out-of-time-ordered correlators and found that the operators grow with a logarithmic “operator cone” in space-time [37–43]. Refs. [22, 23] studied the operator entanglement growth in a MBL system, finding a logarithmic entanglement growth in time. Moreover, in Ref. [44], a lower bound on the Lanczos coefficients is derived for a many-body localized spin chain. Surprisingly, such a lower bound is also shared by a generic chaotic spin chain. Accordingly, the operator growth problem in the Krylov basis and its Krylov complexity certainly warrant studies.

Particularly, we study the operator growth problem in a quantum Ising model with a longitudinal field and random transverse fields. In the strong disordered transverse field limit, the system exhibits many-body localization [45, 46]. We find that, while the Lanczos coefficients in the MBL phase has the same asymptotic behavior as in the ergodic phase, there is an additional even-odd alteration and apparent effective randomness. By numerically calculating the evolution of the corresponding single particle wavefunction hopping on a semi-infinite chain, we found that the Krylov complexity is bounded in time in the MBL phase. Furthermore, we also find that the corresponding single particle hopping problem is localized when initialized on the first site, and therefore the operator is localized in the Krylov subspace.

On the other hand, we also study the operator growth problem in the MBL phenomenological model [47], where the initial operator is a “ l -bit flipping” operator. We find the Lanczos coefficients in this case again show an even-

odd alteration, but approaching to constants asymptotically. We find that the Krylov complexity grows linearly in this case, and the time evolution of the corresponding single particle wavefunction has a traveling wavefront propagating linearly in time.

This paper is organized as follows. In Sec. II, we lay the framework used to study the operator growth using Krylov basis and define different functions of interests including the Krylov complexity. We then discuss the results of operator growth in a MBL system realized in the tilted quantum Ising model in Sec. III, where we show the numerical results and the conjectured behavior of the Lanczos coefficients. Using the Lanczos coefficients, we then calculate the corresponding single particle hopping problem, showing its localization and boundedness of Krylov complexity in time. In Sec. IV, we study the operator growth in the MBL phenomenological model, by calculating the Lanczos coefficients and the Krylov complexity. We conclude in Sec. V with some discussion of our results, open questions and future directions of research.

II. SETUP

We begin by setting up the framework to study the operator growth using Krylov basis. Consider a quantum many-body system described by a Hamiltonian H and an initial local Hermitian operator \mathcal{O} . For the later convenience, we use an operator-state correspondence description: For any operator $\mathcal{O} = \sum_{i,j} O_{ij} |i\rangle\langle j|$, where $|i\rangle$ and $|j\rangle$ are from an orthonormal basis of the Hilbert space of consideration, we can define the corresponding operator state as $|\mathcal{O}\rangle \equiv \sum_{i,j} O_{ij} |i\rangle|j\rangle$. Since we will consider quantities at an infinite temperature, we define the inner product between two operator states $|\mathcal{A}\rangle$ and $|\mathcal{B}\rangle$ as

$$\langle \mathcal{A} | \mathcal{B} \rangle \equiv \frac{\text{Tr}[\mathcal{A}^\dagger \mathcal{B}]}{\text{Tr}[I]}, \quad (1)$$

where I is the identity matrix.

The Heisenberg evolution of an operator is

$$\mathcal{O}(t) = e^{iHt} \mathcal{O} e^{-iHt} = \sum_{n=0}^{\infty} \frac{(it)^n}{n!} \mathcal{L}^n \mathcal{O}, \quad (2)$$

where the Liouvillian superoperator is defined as $\mathcal{L}\mathcal{O} \equiv [H, \mathcal{O}]$. Somewhat abusing the notation, we also define $\mathcal{L}|\mathcal{O}\rangle \equiv [[H, \mathcal{O}]]$. We therefore have, equivalently,

$$|\mathcal{O}(t)\rangle = \sum_{n=0}^{\infty} \frac{(it)^n}{n!} \mathcal{L}^n |\mathcal{O}\rangle. \quad (3)$$

To motivate the Lanczos algorithm, note that we can approximate the Heisenberg evolution Eq. (3) by summing over n up to n_{max} . The resulting approximated operator is therefore in the so-called Krylov space

$$\mathcal{H}_{\mathcal{O}} = \text{span} \{ \mathcal{L}^n |\mathcal{O}\rangle, n = 0 \dots n_{max} \}. \quad (4)$$

Lanczos algorithm generates an orthonormal basis $\{|\mathcal{O}_n\rangle\}$, $n = 0 \dots n_{max}$ of the Krylov space recursively which tridiagonalizes \mathcal{L} . Starting with the initial operator $|\mathcal{O}_0\rangle \equiv |\mathcal{O}\rangle$, we have $|\mathcal{O}_1\rangle = b_1^{-1} \mathcal{L}|\mathcal{O}_0\rangle$, where $b_1^2 = (\mathcal{L}\mathcal{O}_0 | \mathcal{L}\mathcal{O}_0)$. For $n \geq 2$, we recursively define

$$\begin{aligned} |\mathcal{A}_n\rangle &= \mathcal{L}|\mathcal{O}_{n-1}\rangle - b_{n-1}|\mathcal{O}_{n-2}\rangle, \\ b_n^2 &\equiv (\mathcal{A}_n | \mathcal{A}_n), \\ |\mathcal{O}_n\rangle &= \frac{1}{b_n} |\mathcal{A}_n\rangle, \end{aligned} \quad (5)$$

where b_n is the Lanczos coefficient. In this basis, \mathcal{L} becomes tridiagonal with the matrix representation

$$\mathcal{L} = \begin{pmatrix} 0 & b_1 & 0 & 0 & \dots \\ b_1 & 0 & b_2 & 0 & \dots \\ 0 & b_2 & 0 & b_3 & \dots \\ 0 & 0 & b_3 & 0 & \dots \\ \vdots & \vdots & \vdots & \vdots & \ddots \end{pmatrix}. \quad (6)$$

By expanding the operator in the Krylov basis

$$|\mathcal{O}(t)\rangle = \sum_{n=0}^{\infty} \varphi_n(t) |\mathcal{O}_n\rangle, \quad (7)$$

the Heisenberg equation of motion becomes

$$-i\partial_t \varphi_n(t) = b_n \varphi_{n-1}(t) + b_{n+1} \varphi_{n+1}(t), \quad (8)$$

for $n = 0 \dots n_{max}$ with the initial condition $\varphi_n(0) = \delta_{n0}$, where we also define $b_0 \equiv 0$. We therefore see that, the equation of motion governing the coefficients in the Krylov basis can be viewed as a single particle hopping problem on a semi-infinite chain, with the hopping amplitudes b_n 's given by the Lanczos coefficients. Denoting $\vec{\varphi}(t) = (\varphi_0(t), \varphi_1(t), \dots)^T$, we have $\vec{\varphi}(t) = e^{i\mathcal{L}t} \vec{\varphi}(0)$, where $e^{i\mathcal{L}t}$ is the matrix exponential from Eq. (6).

This perspective indeed motivates a natural consideration of complexity. One intuition of the complexity of $|\mathcal{O}(t)\rangle$ comes from the complexity of $|\mathcal{O}_n\rangle$. In particular, $|\mathcal{O}_n\rangle$ involves an n -nested commutator with the Hamiltonian, and the operator is therefore more complex and more nonlocal with the increased order n . The order n therefore can be served as a measure of the operator complexity, which motivates the definition of Krylov complexity in Ref. [25],

$$C_K(t) \equiv \sum_{n=0}^{\infty} n |(\mathcal{O}(t) | \mathcal{O}_n)|^2. \quad (9)$$

It can also be interpreted as the mean position of the particle in the corresponding single particle hopping problem. On the other hand, $\vec{\varphi}(t)$ also gives us a measure of how much resource one has to use to have a good approximation of $|\mathcal{O}(t)\rangle$. If $\vec{\varphi}(t)$ is concentrated or localized at small orders of n , then one does not need too high of a truncation order n_{max} to obtain a good approximation of $|\mathcal{O}(t)\rangle$ in the Lanczos algorithm. As we will see, this is indeed the case for the operators in the MBL systems.

It is worth to mention that, to reconstruct the full information of the operator $|\mathcal{O}(t)\rangle$, one would need both $\bar{\varphi}(t)$ (or equivalently b_n) and $|\mathcal{O}_n\rangle$. However, there are some physical quantities which can be obtained from $\bar{\varphi}(t)$ or b_n solely. The notable ones are the auto-correlation function

$$F(t) \equiv \frac{\text{Tr}[\mathcal{O}(t)^\dagger \mathcal{O}(0)]}{\text{Tr}[I]} = (\mathcal{O}_0 | \mathcal{O}(t)) = \varphi_0(t). \quad (10)$$

The spectral function, defined by its Fourier transformation $\Phi(\omega) = \frac{1}{2\pi} \int_{-\infty}^{\infty} F(t) e^{-i\omega t} dt$, can then be expressed as

$$\Phi(\omega) = \sum_m |(\mathcal{O}_0 | E_m)|^2 \delta(\omega - E_m), \quad (11)$$

where $|E_m\rangle$ is an eigenstate of \mathcal{L} in Eq. (6) with the eigenvalue E_m . We also note that the analytical continuation of the spectral function can also be formally expressed through the continuous fraction of b_n , which is obtained by solving Eq. (8) with Laplace transformation [25, 48].

III. OPERATOR GROWTH IN A MBL SYSTEM

In this section, we study the operator growth problem from the perspective of Lanczos algorithm in a MBL system. We consider a 1d spin chain with L sites with an open boundary condition

$$H = -J \sum_{\langle ij \rangle} Z_i Z_j - g \sum_j X_j + \sum_j h_j Z_j, \quad (12)$$

where $\langle ij \rangle$ denotes the nearest neighbors, X_j, Y_j, Z_j are the Pauli matrices on site j , $J = 1$ is the energy unit, $g = -1.05$ and h_i is the random transverse field drawing from a uniform distribution $[-h, h]$. (For an odd chain, we consider sites $j = -(L-1)/2 \dots (L-1)/2$; for an even chain, we consider sites $j = -L/2+1 \dots L/2$.) Such a spin chain exhibits MBL when the disorder strength $h \gtrsim 3$ as shown in Appendix A. For all of our following calculations, we generate 10^3 disorder realizations, and all the disorder-averaged quantities are denoted with an overline.

A. Lanczos coefficients

First we generate the Lanczos coefficients and examine their behaviors for various disorder strengths h . In Fig. 1, we show the disorder averaged Lanczos coefficients in a system size $L = 13$ with the initial operator $\mathcal{O}_0 = Z_{j=0}$. We note that before the saturation or the plateau at large n , \bar{b}_n appears to have an asymptotic behavior $\sim n/\ln(n)$, consistent with Refs. [25, 44]. In the linear-linear plot (Fig. 2), the traces indeed appear to be linear and the

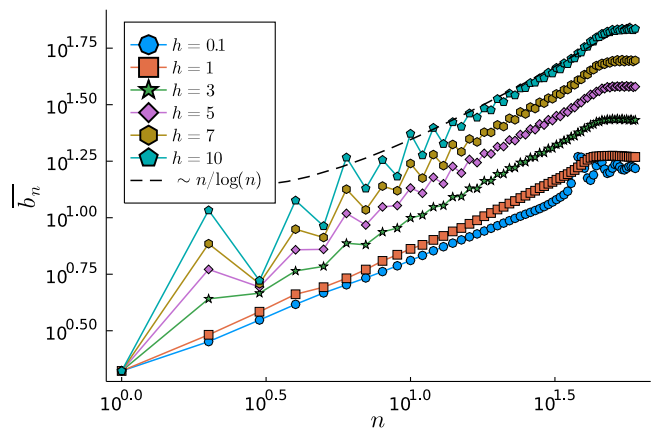


FIG. 1. Disorder-averaged Lanczos coefficients \bar{b}_n for several disorder strengths h in the tilted quantum Ising model Eq. (12), starting with the Z_0 initial operator and system size $L = 13$. In the MBL phase $h \gtrsim 3$, \bar{b}_n has the same asymptotic behavior as in the ergodic phase, but with an additional even-odd alteration.

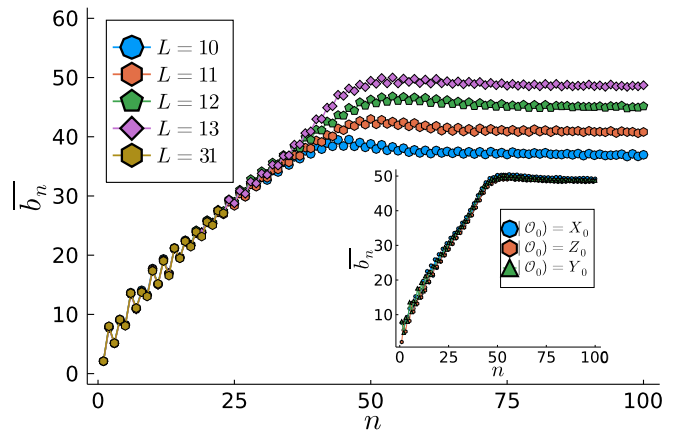


FIG. 2. Disorder-averaged Lanczos coefficients \bar{b}_n for several system sizes L and $h = 7$, with the initial operator Z_0 . The onset point of the plateau of \bar{b}_n increases with the system size L . We therefore conclude that the saturation of \bar{b}_n is due to the finite size. Inset: the disorder averaged Lanczos coefficients starting with the the X_0, Y_0 and Z_0 operators. The observed even-odd alteration of the Lanczos coefficients is independent of the choice of the initial operators.

logarithmic correction is difficult to notice. However, as we see in the log-log plot in Fig. 1, the logarithmic correction has the effect of skewing the apparent exponent $b_n \sim n^\delta$ of δ from $\delta = 1$ to $\delta \approx 0.8$. We also plot our data with $\sim n/\ln(n)$ to show that the logarithmic correction is indeed present, and such a behavior is expected in both the MBL and ergodic phases. On the other hand, we observe that in the MBL phase $h \gtrsim 3$, the averaged Lanczos coefficients b_n starts to show an even-odd alteration, with the amplitude of the alteration increases with an increased disorder strength h .

In Fig. 2, we plotted \bar{b}_n generated from different sys-

tem sizes. We see that the starting n of the saturation or plateau increases as the system size L increases. We therefore conclude that the plateau behavior of \bar{b}_n is due to the finite system size L . In fact, this appears to be a common finite-size feature of the Lanczos coefficients in various models [31, 48].

To further confirm that the data before the plateau is representative of the thermodynamic limit, we push the calculation up to $L = 31$ using a different algorithm which uses the product of Pauli matrices as the basis and only tracks the coefficients. This enables a large L computation, but can only allow calculation to reach smaller n since it requires exponentially more resources to represent $|\mathcal{O}_n\rangle$ with increasing n . We note that the Lanczos coefficients for $L = 31$ show the same behavior for small n as the smaller system sizes. This again supports our conclusion that the asymptotic scaling and the even-odd alteration of Lanczos coefficients before the saturation is representative of the thermodynamic limit. In the inset of Fig. 2, we also show that the aforementioned observed behaviors of b_n is independent of the initial local operator.

With the above observations, the mathematical results in Ref. [44] (despite the different choice of the disorder distribution), and looking at several disorder realizations of b_n such as the ones shown in Fig. 3, we conjecture the Lanczos coefficients in the MBL system will have the following asymptotic behavior:

$$b_n = \begin{cases} a_e \frac{n}{\ln n} + c_e + \Gamma_n, & \text{if } n \text{ even} \\ a_o \frac{n}{\ln n} + c_o + \Gamma_n, & \text{if } n \text{ odd} . \end{cases} \quad (13)$$

More precisely, by the above formula, we expect the parameters $a_{e(o)}$ and $c_{e(o)}$ to be different for *each disorder realization*, drawing from some probability distributions. On the other hand, we also expect an additional effective randomness Γ_n for each n , drawing from a probability distribution independent of n .

To further verify our conjectured formula, for each disorder realization, we take the Lanczos coefficients in the range $n = 10$ to $n = 40$ and fit them with $y_{\text{fit}} = a_{e(o)}n/\ln n + c_{e(o)}$ using least-square fit for the even and odd branch respectively. The resulting fits are shown in Fig. 3 for some disorder realizations and the histogram of the fitted parameters are shown in Fig. 4 (a)-(d). After fitting the data, we then examine the difference between the data and the fit $y - y_{\text{fit}}$ and plot the histogram of the differences collected from each n in $n = 10$ to $n = 40$ from both even and odd branch, as shown in Fig. 4(e). We see that the histograms in Fig. 4 all look very close to Gaussian distributions, which supports our conjecture that these parameters can be viewed as drawing from some probability distributions independently, and the means and variances of the probability distributions can be estimated from the Gaussian distributions shown in Fig. 4, according to the central limit theorem.

An advantage of using recursive method or the Lanczos algorithm is that it allows us to extrapolate the Lanczos

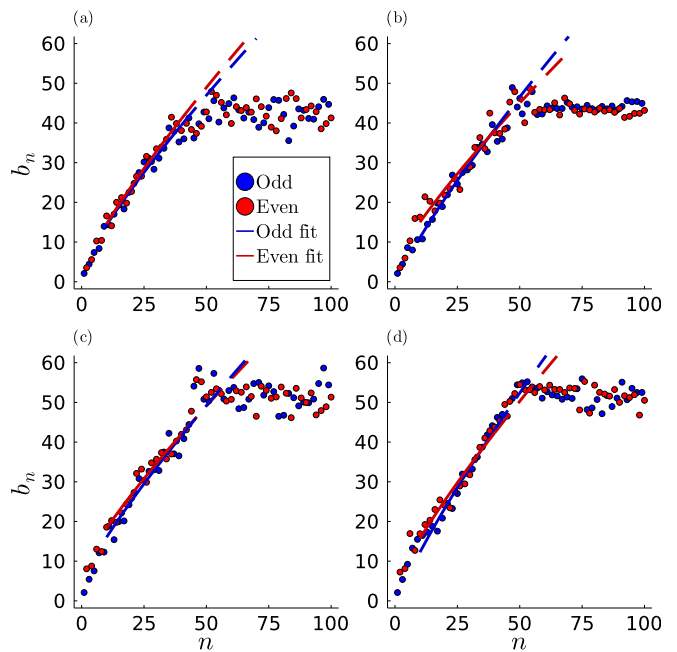


FIG. 3. (a)-(d) Disorder realizations of the Lanczos coefficients for Eq. (12), with the initial operator Z_0 , $h = 7$ and $L = 13$. We use the data points in the range of $n = 10$ to $n = 40$ to fit the conjectured asymptotic behavior of the Lanczos coefficients Eq. (13), and then use the fitted results to extrapolate the Lanczos coefficients for $n > 40$ for each realization.

coefficients in an attempt to assert some quantities such as the spectral function in the thermodynamic limit with various extrapolation schemes [25, 48, 49]. With the conjectured asymptotic behavior Eq. (13), we extrapolate the Lanczos coefficients to large n and to the thermodynamic limit using the following scheme. For each disorder realization of b_n , we obtained the fitted parameters of $a_{e(o)}$ and $c_{e(o)}$ from fitting the data in the range $n = 10$ to $n = 40$ as mentioned previously. We then take these numerical results up to $n = 40$, and then extrapolate b_n for $n > 40$ to $n_{\text{max}} = 1000$ using Eq. (13) with the fitted $a_{e(o)}$ and $c_{e(o)}$ for this realization and the randomness Γ_n drawing from a Gaussian ensemble with the mean and the variance given by the parameters in Fig. 4(e). In the following, we will study various quantities using the unextrapolated b_n (usually denoted by solid lines in the figures) and using the extrapolated b_n (usually denoted by dashed lines in the figures).

B. Spectral Function

First let us examine the behavior of the spectral function using Eq. (11). In terms of the corresponding single particle hopping problem, the spectral function is just the density of states weighted by the weight function which is the probability of the eigenfunction on the first site

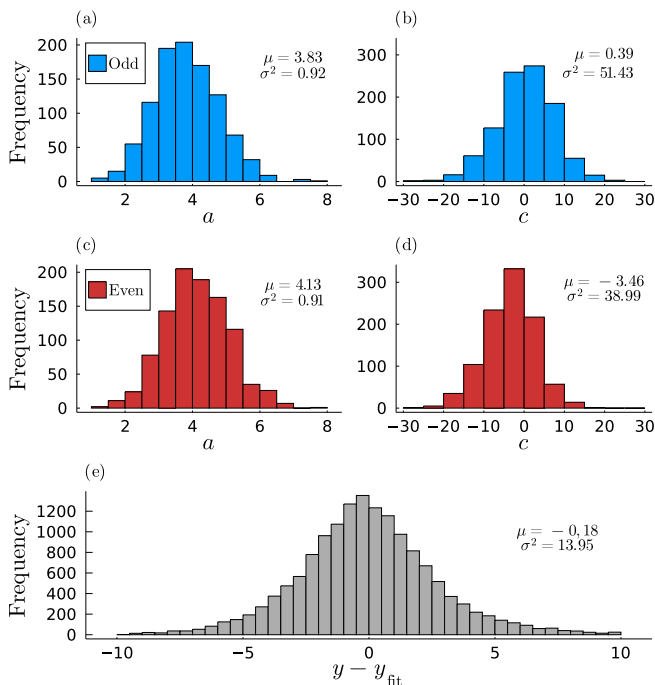


FIG. 4. (a)(b) The histograms of the fitted parameters a_o and c_o from Eq. (13) on the odd branch. (c)(d) The histograms of the fitted data a_e and c_e from the even branch. (e) The histogram of Γ_n in Eq. (13), obtained by taking the difference between the data and the fitted results $y - y_{\text{fit}}$, where $y_{\text{fit}} = a_{o(e)}n/\ln(n) + c_{o(e)}$ with the fitted parameter for each realization. The Gaussian distributions of the histogram supports the conjectured effective randomness of the parameters.

$|\langle \mathcal{O}_0 | E_j \rangle|^2$ and therefore can be obtained by diagonalizing Eq. (6). Our attempt is to extract the analytical behavior at low and high frequencies in the thermodynamic limit. Since numerically, one can only obtain discrete eigenvalues from diagonalizing Eq. (6), the spectral function will be a sum of delta functions with some weights. It is therefore more customary to consider the cumulative spectral function

$$\chi(\omega) \equiv \int_{\Omega=-\infty}^{\omega} \Phi(\Omega) d\Omega = \sum_{E_j < \omega} |\langle \mathcal{O}_0 | E_j \rangle|^2, \quad (14)$$

and extract the smooth part of the cumulative spectral function. This also gives us a convenient way to average over disorder realizations, where one would just sum over all the weights below ω in Eq. (14) from all the disorder realizations and then divide it by the number of realizations.

We examine the high frequency behavior of $\bar{\chi}(\omega)$ first, using the unextrapolated and extrapolated b_n . In Ref. [25], it was proposed that if the Lanczos coefficients grows linearly in n , then the spectral function at the high frequencies decays exponentially $\Phi(\omega) \sim \exp(-\frac{\pi|\omega|}{2\alpha})$, where α is the coefficient of the linear growth $b_n \sim \alpha n$. Since $\bar{\chi}(\omega \rightarrow \infty) = 1$, we plot $1 - \bar{\chi}(\omega \rightarrow \infty)$ as shown in Fig. 5. From the figure, we see that at high

frequency, $\bar{\chi}(\omega)$ decays exponentially, and therefore so does $\Phi(\omega)$ for both the unextrapolated and extrapolated b_n . Furthermore, we extract the exponential decay as $\chi(\omega) \sim \exp(-\frac{\pi\omega}{2\alpha})$, where $\alpha \approx 4.36$, which is close to the mean values of $a_{e(o)}$ as shown in Fig. 4. We see that the high frequency behavior of the spectral function is indeed blind to the MBL or ergodic phase [44].

On the other hand, at the zero frequency, we observe the presence of a delta function in the spectral function $\Phi(\omega) \sim A\delta(\omega) + \dots$ (manifested as a step function for the cumulative spectral function $\chi(\omega)$) for the unextrapolated data $n_{\text{max}} = 40$ and also for the extrapolated data. The existence of the delta function is indeed a hallmark of MBL, since it implies that the auto-correlation function $F(t)$ will decay to $A \neq 0$ at infinite time, assuming the rest part of the spectral function is analytical. These results also suggest that our extrapolation scheme is reasonable, since it does not change the expected qualitative behaviors of the spectral function in MBL.

It is also interesting to see if the spectral function shows any singular behavior at low frequencies in addition to the zero-frequency delta function. The low-frequency singular behavior of the spectral function would manifest in the long-time behavior of the auto-correlation function. While not shown in the figure, we attempt to fit the low frequency part of the cumulative spectral function using the $n_{\text{max}} = 1000$ result with $\omega^{\gamma+1}$ and found that $\gamma \approx 0.39$ (so that $\Phi(\omega) \sim \omega^{0.39}$). However, we note that it is still fairly challenging to extract the low-frequency singular behavior from our present numerical data. It would be ideal if one can obtain an analytical low-frequency result from the physics of MBL or from our conjectured asymptotic formula Eq. (13) and to compare with our disorder-averaged spectral function [50–55]. On the other hand, if one has an expected low-frequency behavior of the spectral function, one can also use this information to modify the conjectured behavior of b_n [48, 49]. In any case, the low-frequency behavior of the spectral function in MBL warrants a further investigation in the future using the recursive method [49].

C. Krylov complexity

As discussed in the Sec. II, we can view the operator growth problem as a single particle hopping problem on a semi-infinite chain. The time evolution of the single particle wavefunction $\vec{\varphi}(t)$ therefore reflects the growth of the operator in the Krylov basis $|\mathcal{O}(t)\rangle = \sum_n \varphi_n(t) |\mathcal{O}_n\rangle$.

First, we examine the mean position of the corresponding single particle wavefunction, namely the Krylov complexity, from both unextrapolated and extrapolated b_n . In Fig. 6, we show the disorder-averaged Krylov complexity in the MBL phase ($h = 7$) in time. The long-time averaged Krylov complexity appears to be bounded in time and saturates quickly to a value much smaller than the truncation n_{max} from both extrapolated and unextrap-

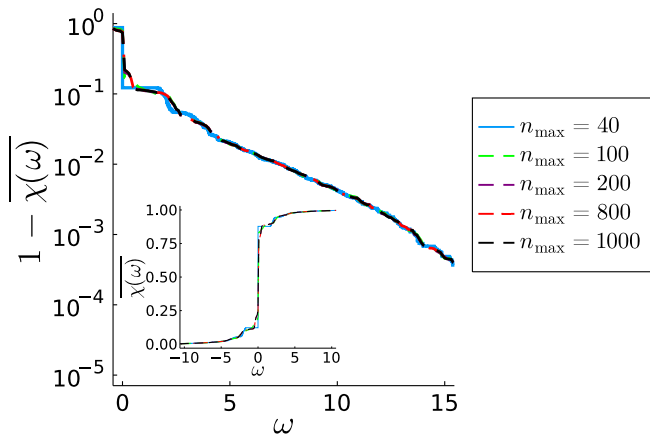


FIG. 5. The disorder-averaged cumulative spectral function $\overline{\chi(\omega)}$. The high frequency behavior appears to decay exponentially, regardless of calculated from the unextrapolated b_n with $n_{\max} = 40$ or from the extrapolated b_n with $n_{\max} > 40$. Note that the cumulative spectral function appears to be converged when $n_{\max} = 200$. Inset: the overall disorder-averaged cumulative spectral function $\overline{\chi(\omega)}$. Note that the existence of $\delta(\omega)$ in the spectral function, a hallmark of many-body localization, is unaffected by our extrapolation scheme of the Lanczos coefficients.

olated b_n . Note that $\overline{C_K(t)}$ shows a fluctuation around the long-time averaged value at long time, and the magnitude of the fluctuation appears to grow logarithmically in time. However, by examining $C_K(t)$ for several n_{\max} , we notice the onset time of such a fluctuation increases with n_{\max} , suggesting it as a result of finite n_{\max} . We therefore conclude that the Krylov complexity is bounded in time in MBL systems.

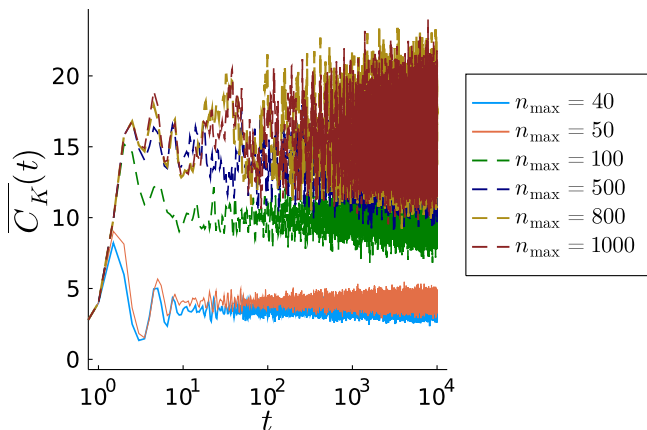


FIG. 6. Disorder-averaged Krylov complexity $C_K(t)$ in MBL ($h = 7$) from the unextrapolated Lanczos coefficients (solid lines) and from the extrapolated Lanczos coefficients (dashed lines). The Krylov complexity $C_K(t)$ appears to be bounded in time and we expect the fluctuations in time at the long times are due to finite n_{\max} . Note that in any case, the truncation n_{\max} is much greater than $C_K(t)$.

The growth of the operator can be more easily visu-

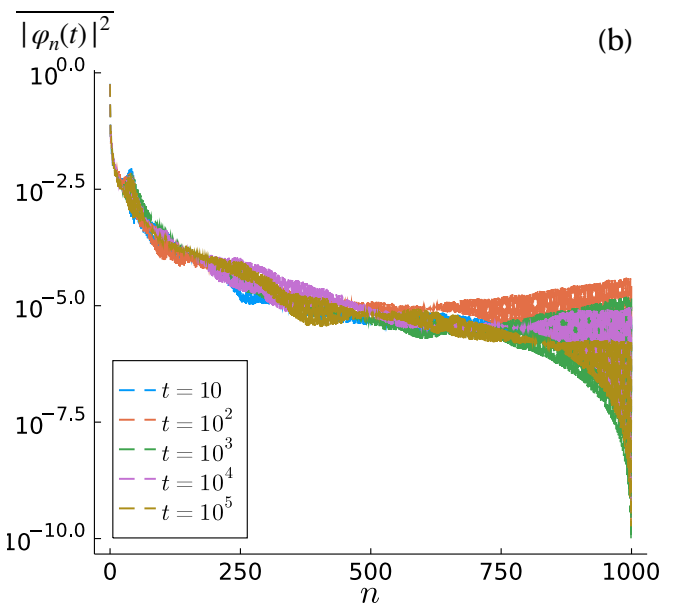
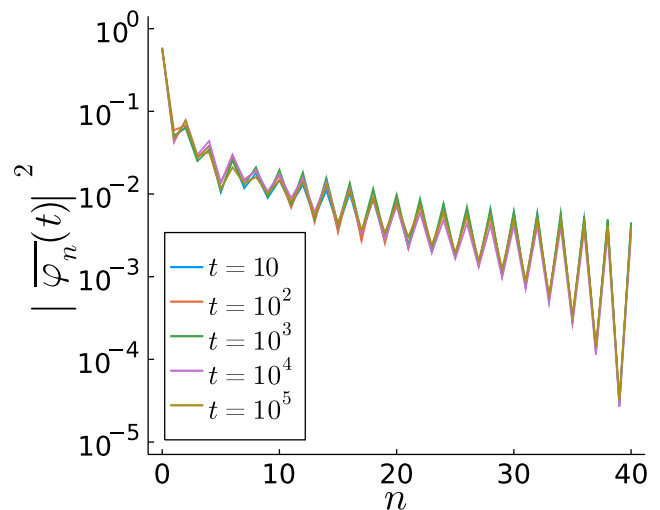


FIG. 7. Disorder-averaged probability distribution $|\overline{\varphi_n(t)}|^2$ in the MBL phase $h = 7$ at different times from (a) unextrapolated b_n with $n_{\max} = 40$ and (b) extrapolated b_n with $n_{\max} = 1000$. The wavefunctions appear to be localized at small n even at large times.

alized by examining the probability distribution of the single particle wavefunction at various times. In Fig. 7, we show $|\overline{\varphi_n(t)}|^2$ from both unextrapolated and extrapolated Lanczos coefficients. Remarkably, we see the wavefunctions are localized around the first site even for an exponentially long time. We therefore conclude that the corresponding single particle hopping problem in the MBL phase is localized if initialized on the first site. This is in stark contrast with the case in the ergodic phase, where the single particle wavefunction propagates to large n superpolynomially fast [25].

Our result also implies that the Krylov method can be an efficient method to simulate the operator dynamics in MBL. In practice, we have to choose a truncation

n_{\max} as the cut-off order of the Lanczos algorithm. If $\varphi_n(t)$ is localized at small n , then the truncation error $\epsilon(t) = \sum_{n=n_{\max}+1}^{\infty} |\varphi_n(t)|^2$ will be small. In particular, from our results of $|\varphi_n(t)|^2$, we expect this error will be small for MBL systems even at exponentially long times. Note that while $|\varphi_n(t)|^2$ seems to be localized and not changing too much with times, the phases are still evolving. This can still cause the operator entanglement entropy or out-of-time-ordered correlator to change at long times in MBL systems.

IV. OPERATOR GROWTH IN THE MBL PHENOMENOLOGICAL MODEL

In this section, we study the operator growth and the Krylov complexity in the MBL phenomenological model [47] to compare with the results in the previous section. A defining feature of the MBL system is the existence of the local integrals of motion [56, 57], namely the “ ℓ -bits”, resulting in the following phenomenological model

$$H_{\text{ph}} = \sum_j J_j^{(0)} \hat{\tau}_j^z + \sum_{i<j} J_{ij}^{(1)} \hat{\tau}_i^z \hat{\tau}_j^z + \sum_{n=2} \sum_{i<j, \{k\}} J_{i\{k\}j}^{(n)} \hat{\tau}_i^z \hat{\tau}_{k_1}^z \cdots \hat{\tau}_{k_{n-1}}^z \hat{\tau}_j^z, \quad (15)$$

where $\{k\}$ denotes the set of sites $i < k_1, \dots, k_{n-1} < j$, $\hat{\tau}_j^z$ are the ℓ -bits which can be related to the physical bits Z_j by the unitary which diagonalizes the Hamiltonian, and $J_{ij}^{(2)}$ and $J_{i\{k\}j}^{(n)}$ are the interactions among the ℓ -bits which decays exponentially in the number of ℓ -bits involved and the distances between the ℓ -bit. To simplify the problem, we assume $J_{i\{k\}j}^{(n)} = K_{i\{k\}j}^{(n)} \exp(-nr/\xi)$ (including $n=0$ and 1), where the range $r = j - i$, ξ being the localization length, and the parameters $K_{i\{k\}j}^{(n)}$ are drawing from an uniform distribution $[-W, W]$ [22, 41]. In particular, we consider the parameters $L = 13$ as the system size, $\xi = 0.6$ and $W = 5.0$, with 10^3 disorder realizations.

A. Lanczos coefficients

Here we generate the Lanczos coefficients from the Hamiltonian Eq. (15) with the initial operator $\mathcal{O}_0 = \hat{\tau}_0^x$. To calculate the Lanczos coefficients, it is easy to split the Hamiltonian to a part that involves τ_0^z and the rest: $H_{\text{ph}} = J_{\text{eff}} \tau_0^z + H_{\text{other}}$, where

$$J_{\text{eff}} = J_0^{(0)} + \sum_{j \neq 0} J_{0j}^{(1)} \tau_j^z + \sum_{n=2}^{L-1} \sum_{\{j\} \neq 0} J_{0\{j\}}^{(n)} \tau_{j_1}^z \cdots \tau_{j_n}^z. \quad (16)$$

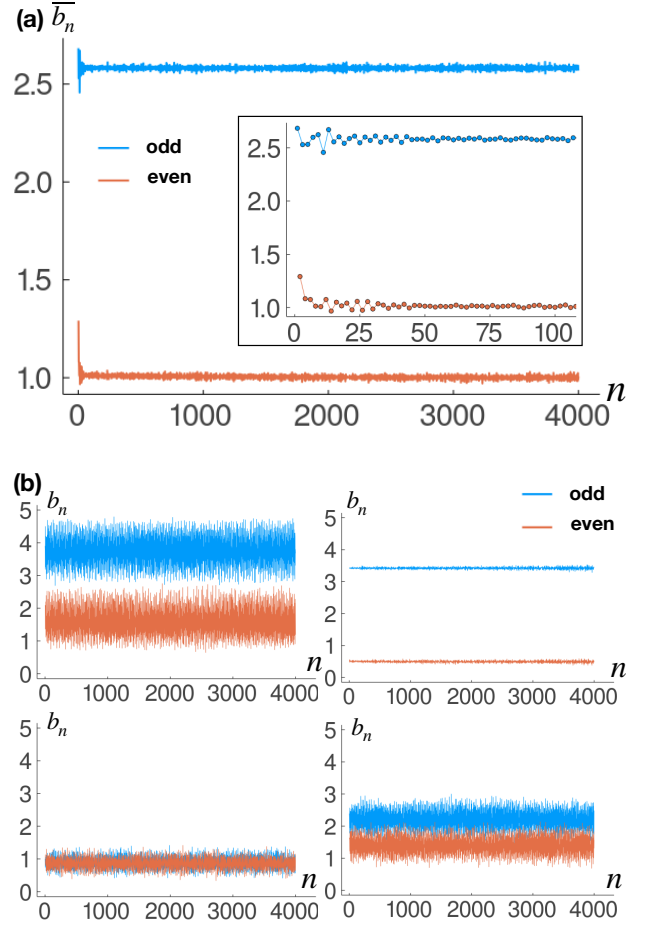


FIG. 8. (a) The disorder-averaged Lanczos coefficients $\overline{b_n}$ from the MBL phenomenological model Eq. (15) with the initial operator τ_0^x . The Lanczos coefficients have an even-odd alteration, both approaching to a constant in large n . Inset: The disorder averaged Lanczos coefficients $\overline{b_n}$ at small n . (b) The Lanczos coefficients b_n from the MBL phenomenological model for several disorder realizations.

It is easy to see that $J_{\text{eff}} \tau^z$ is indeed the only part that generates the Heisenberg evolution of τ_0^x . In fact, one can obtain $\mathcal{L}^{2n-1} \tau_0^x = i \tau_0^y (J_{\text{eff}})^{2n-1}$ and $\mathcal{L}^{2n} \tau_0^x = \tau_0^x (J_{\text{eff}})^{2n}$. By expressing J_{eff} as a diagonal matrix with a dimension $2^{L-1} \times 2^{L-1}$ where the entries corresponding to different τ^z configurations, we obtain the following recursive method to generate the Lanczos coefficients: Define $B_0 = I$ as a $2^{L-1} \times 2^{L-1}$ identity matrix, $B_1 = J_{\text{eff}}$, $b_0 = 1$ and $b_1^2 = \frac{1}{2^L} \text{Tr}[B_1^2]$, then

$$B_{n+1} = \frac{1}{b_n} J_{\text{eff}} B_n - \frac{b_n}{b_{n-1}} B_{n-1}, \quad (17)$$

$$b_{n+1}^2 = \frac{1}{2^L} \text{Tr}[B_{n+1}^2],$$

for $n > 1$. This gives us $O_{2n-1} = b_{2n-1}^{-1} i \tau_0^y B_{2n-1}$ and $O_{2n} = b_{2n}^{-1} \tau_0^x B_{2n}$ from the Lanczos algorithm.

In Fig. 8(a), we show the disorder averaged Lanczos

coefficients $\overline{b_n}$ from the phenomenological model. Note that $\overline{b_n}$ appears to approach a constant, but also with an even-odd alteration and the odd branch usually has a higher value than the even branch. We also show several disorder realizations of b_n in Fig. 8(b).

B. Krylov Complexity

For each disorder realization of b_n , we can solve for the corresponding single particle dynamics, representing its operator growth. In Fig. 9, we plotted the disorder averaged Krylov complexity $\overline{C_K(t)}$ of MBL phenomenological model. We notice that, after $t \gtrsim 1$, the Krylov complexity appears to grow linearly in time and saturate. However, by plotting $\overline{C_K(t)}$ with several different n_{max} , we conclude that the saturation is due to the finite- n_{max} , and therefore we expect the linearly growing behavior of $\overline{C_K(t)}$ will continue in the true $n_{max} \rightarrow \infty$ limit.

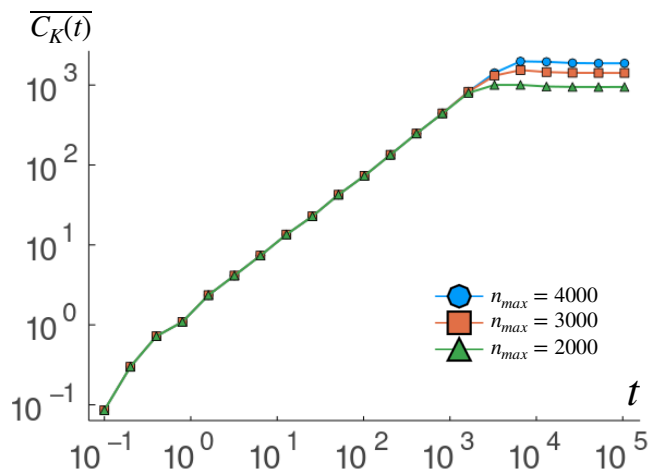


FIG. 9. The disorder averaged Krylov complexity $\overline{C_K(t)}$ in the MBL phenomenological model. After a short time, $\overline{C_K(t)}$ appears to grow linearly in time before it reaches the saturation. By comparing the results with several n_{max} , we conclude that the saturation is a finite- n_{max} effect.

The operator growth in the Krylov basis can be even better visualized by looking at $|\overline{\varphi_n(t)}|^2$ at different times, which we plotted in Fig. 10. As we can see, the wavefunction has a feature of a propagating “wavefront” towards large n , which appears to propagate linearly in time. The time scale where the “wavefront” hits n_{max} is also the time scale $\overline{C_K(t)}$ starts to saturate. It is therefore clear that the saturation of $\overline{C_K(t)}$ is indeed a finite- n_{max} effect, and the single particle wavefunction $\overline{\varphi(t)}$ will propagate indefinitely in the $n_{max} \rightarrow \infty$ limit. This is in stark contrast with the growth of the “p-bit” shown in Sec. III, where the operator appears to be localized.

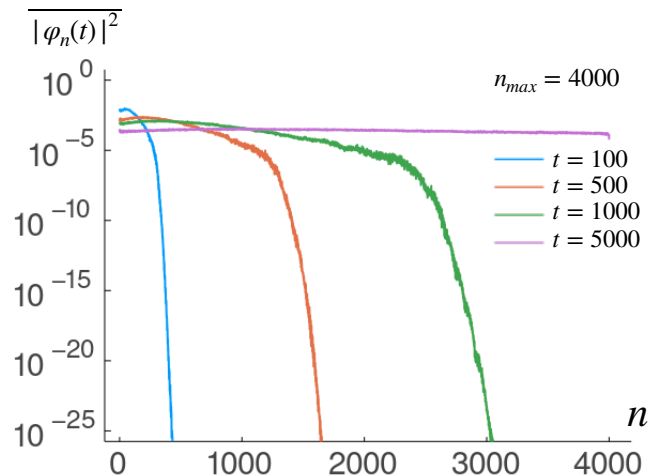


FIG. 10. The disorder averaged probability distribution $|\overline{\varphi_n(t)}|^2$ at different times. The wavefunction has a propagating wavefront, where the wavefront appears to propagate towards higher n linearly in time.

V. CONCLUSIONS

In this paper, we study the operator growth problem in a MBL system using Krylov basis. From this point of view, the operator growth problem can be mapped to a single-particle hopping problem on a semi-infinite chain with the hopping amplitudes given by the Lanczos coefficients. In particular, we consider the problem with the initial operators as a “p-bit” (X_0) and as an “ ℓ -bit” (τ_0^x). We find that, in the “p-bit” case, the asymptotic behavior of the Lanczos coefficients behaves as $b_n \sim n/\log(n)$, same as in the ergodic case. However, the presence of the even-odd alteration and relatively strong effective randomness are the features that are distinguishable from the ergodic phase. These features could potentially be used as an alternative diagnostic for MBL. It is worth to mention that, we also examine the Lanczos coefficients in the MBL system realized by a Heisenberg chain (shown elsewhere [58]). We find that the aforementioned features are still present, and therefore we conclude that these features are generic for MBL and independent of the choices of the model. On the other hand, for the “ ℓ -bit”, the Lanczos coefficients also show an even-odd alteration, but approach to constants at large n , in contrast with the results for the “p-bit”.

With our conjectured asymptotic behavior of the Lanczos coefficients in MBL for the “p-bit”, we extrapolate the Lanczos coefficients to the thermodynamic limit, and study the spectral function from the resulting extrapolated Lanczos coefficients. We found that the existence of the delta function at zero frequency, which is a hallmark of MBL phase, is unaffected by our extrapolation. Moreover, we also show that the spectral function decays exponentially at high frequencies. The low-frequency behavior of the spectral function is more challenging to ex-

tract. It is therefore interesting to see if the conjectured asymptotic Lanczos coefficients can provide us some analytical understanding of the low-frequency asymptotic behavior of the spectral function.

Perhaps somewhat surprisingly, even though the asymptotic behaviour of the Lanczos coefficients are the same in both MBL and ergodic phases, the corresponding single particle hopping problem is localized in the MBL phase if initialized on the first site, resulting in a bounded Krylov complexity in time. Note that we show this for both extrapolated and unextrpolated Lanczos coefficients. In contrast, the Krylov complexity in the ergodic phase grows superpolynomially in time [25], corresponding to the delocalization of the single particle. On the other hand, the Krylov complexity for “ ℓ -bit” grows linearly in time, due to the different choices of the Krylov basis.

We comment on some questions and future directions motivated from our results. As our results have shown, the single particle hopping problem is localized when initialized on the first site in MBL phase but propagates superpolynomially fast and therefore is delocalized in the ergodic phase. From this perspective, can we study or understand the MBL-ergodic transition from this corresponding single particle localization-delocalization transition? It would also be interesting to understand the properties of the spectral function or auto-correlation function at the MBL transition from this point of view, and to deepen our understanding of possible experimental signatures of MBL-ergodic transition.

Since in the MBL phase, the operator is exponentially localized in the Krylov space even at long times, Lanczos algorithm is a good method to obtain the operator dynamics. In other words, one does not need too high of a truncation n_{\max} to obtain a good approximation of $|\mathcal{O}(t)\rangle$. However, we note that even in the MBL case, it can still require exponential resources to represent $|\mathcal{O}_n\rangle$. Can we design a Krylov-based numerical method to simulate the MBL dynamics more efficiently? Some Krylov-based hybrid numerical methods might be possibilities to alleviate the obstacle, enabling us to simulate MBL dynamics efficiently in larger system sizes and longer times on a classical computer.

Finally, our result suggests a correspondence of the “dynamical phases” and “computational complexity”. That is to say, the complexity of using Krylov method to calculate the operator dynamics is low for systems in MBL phase, independent of the microscopic model. It is therefore interesting to see how much of this correspondence holds for different types of the dynamical phase. Analogous to the recent developments of using computational complexity to understand and characterize different phases of matters, our results could suggest a new fruitful direction of using complexity to understand and characterize dynamical phases.

ACKNOWLEDGMENTS

We thank Timothy Hsieh and LiuJun Zou for the valuable discussions. We acknowledge supports from Perimeter Institute for Theoretical Physics. Fabian Ballar Trigueros would like to thank the PSI program for facilitating this research. Research at Perimeter Institute is supported in part by the Government of Canada through the Department of Innovation, Science and Economic Development Canada and by the Province of Ontario through the Ministry of Colleges and Universities.

Appendix A: Gap ratio statistics of the random tilted Ising model

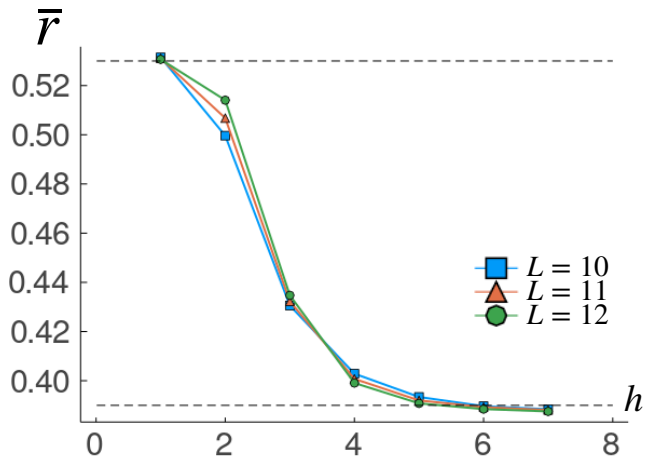


FIG. 11. The gap ratio statistics r for various disorder strength h and system size L . Note that the dashed lines correspond to the mean values from a Gaussian orthogonal ensemble ($\bar{r} \approx 0.53$) and a Poisson ensemble ($\bar{r} \approx 0.39$). We therefore see that the system is in MBL when $h \gtrsim 3$.

In this appendix, we show the gap ratio statistics [35] for the tilted quantum Ising model Eq. (12). In particular, we define $r = \min(\delta_n, \delta_{n-1}) / \max(\delta_n, \delta_{n-1})$, where $\delta_n = E_{n+1} - E_n$ is the energy difference between two consecutive eigenstates. We take the middle half of the spectrum to calculate the mean value of r , and then average over 10^3 disorder realizations to obtain \bar{r} for various disorder strength h and system size L , plotted in Fig. (11). Note that for the Gaussian orthogonal ensemble, one expects $\bar{r} \approx 0.53$ while $\bar{r} \approx 0.39$ for the Poisson distribution. We therefore see that, for the Hamiltonian Eq. (12), $h \gtrsim 3$ is the regime where the system is in the many-body localization phase.

-
- [1] Alexei Kitaev, “A Simple Model of Quantum Holography,” (2015).
- [2] Juan Maldacena, Stephen H. Shenker, and Douglas Stanford, “A Bound on Chaos,” *J. High Energy Phys.* **2016**, 106 (2016).
- [3] Alexei Kitaev and S. Josephine Suh, “The Soft Mode in the Sachdev-Ye-Kitaev Model and Its Gravity Dual,” *J. High Energy Phys.* **2018**, 183 (2018).
- [4] Daniel A. Roberts, Douglas Stanford, and Alexandre Streicher, “Operator growth in the SYK model,” *J. High Energy Phys.* **2018**, 122 (2018).
- [5] C. W. von Keyserlingk, Tibor Rakovszky, Frank Pollmann, and S. L. Sondhi, “Operator hydrodynamics, OTOCs, and entanglement growth in systems without conservation laws,” *Phys. Rev. X* **8**, 021013 (2018).
- [6] Adam Nahum, Sagar Vijay, and Jeongwan Haah, “Operator spreading in random unitary circuits,” *Phys. Rev. X* **8**, 021014 (2018).
- [7] Igor L. Aleiner, Lara Faoro, and Lev B. Ioffe, “Microscopic Model of Quantum Butterfly Effect: Out-of-Time-Order Correlators and Traveling Combustion Waves,” *Ann. Phys.* **375**, 378–406 (2016).
- [8] Debanjan Chowdhury and Brian Swingle, “Onset of many-body chaos in the $O(N)$ model,” *Phys. Rev. D* **96**, 065005 (2017).
- [9] Martin Gärttner, Justin G. Bohnet, Arghavan Safavi-Naini, Michael L. Wall, John J. Bollinger, and Ana Maria Rey, “Measuring Out-of-Time-Order Correlations and Multiple Quantum Spectra in a Trapped-Ion Quantum Magnet,” *Nat. Phys.* **13**, 781–786 (2017).
- [10] Jun Li, Ruihua Fan, Hengyan Wang, Bingtian Ye, Bei Zeng, Hui Zhai, Xinhua Peng, and Jiangfeng Du, “Measuring Out-of-Time-Order Correlators on a Nuclear Magnetic Resonance Quantum Simulator,” *Phys. Rev. X* **7**, 031011 (2017).
- [11] Cheng-Ju Lin and Olexei I. Motrunich, “Out-of-time-ordered correlators in a quantum Ising chain,” *Phys. Rev. B* **97**, 144304 (2018).
- [12] Cheng-Ju Lin and Olexei I. Motrunich, “Out-of-time-ordered correlators in short-range and long-range hardcore boson models and in the Luttinger-liquid model,” *Phys. Rev. B* **98**, 134305 (2018).
- [13] Sarang Gopalakrishnan, “Operator Growth and Eigenstate Entanglement in an Interacting Integrable Floquet System,” *Phys. Rev. B* **98**, 060302 (2018).
- [14] Vedika Khemani, David A. Huse, and Adam Nahum, “Velocity-dependent Lyapunov exponents in many-body quantum, semiclassical, and classical chaos,” *Phys. Rev. B* **98**, 144304 (2018).
- [15] Shenglong Xu and Brian Swingle, “Accessing scrambling using matrix product operators,” *Nature Physics* **16**, 199–204 (2020).
- [16] Christoph Sünderhauf, Lorenzo Piroli, Xiao-Liang Qi, Norbert Schuch, and J. Ignacio Cirac, “Quantum chaos in the Brownian SYK model with large finite N : OTOCs and tripartite information,” *J. High Energy Phys.* **2019**, 38 (2019).
- [17] Bin Yan, Lukasz Cincio, and Wojciech H. Zurek, “Information scrambling and loschmidt echo,” *Phys. Rev. Lett.* **124**, 160603 (2020).
- [18] Tomaž Prosen and Iztok Pizorn, “Operator space entanglement entropy in a transverse Ising chain,” *Phys. Rev. A* **76**, 032316 (2007).
- [19] Iztok Pizorn and Tomaž Prosen, “Operator space entanglement entropy in XY spin chains,” *Phys. Rev. B* **79**, 184416 (2009).
- [20] V. Alba, J. Dubail, and M. Medenjak, “Operator entanglement in interacting integrable quantum systems: The case of the rule 54 chain,” *Phys. Rev. Lett.* **122**, 250603 (2019).
- [21] Bruno Bertini, Pavel Kos, and Tomaz Prosen, “Operator entanglement in local quantum circuits I: Chaotic dual-unitary circuits,” *SciPost Phys.* **8**, 67 (2020).
- [22] Ian MacCormack, Mao Tian Tan, Jonah Kudler-Flam, and Shinsei Ryu, “Operator and entanglement growth in non-thermalizing systems: Many-body localization and the random singlet phase,” [arXiv:2001.08222](https://arxiv.org/abs/2001.08222).
- [23] Eric Mascot, Masahiro Nozaki, and Masaki Tezuka, “Local Operator Entanglement in Spin Chains,” [arXiv:2012.14609](https://arxiv.org/abs/2012.14609).
- [24] Vincenzo Alba, “Diffusion and operator entanglement spreading,” *Phys. Rev. B* **104**, 094410 (2021).
- [25] Daniel E. Parker, Xiangyu Cao, Alexander Avdoshkin, Thomas Scaffidi, and Ehud Altman, “A Universal Operator Growth Hypothesis,” *Phys. Rev. X* **9**, 041017 (2019).
- [26] E. Rabinovici, A. Sánchez-Garrido, R. Shir, and J. Sonner, “Operator complexity: A journey to the edge of Krylov space,” *Journal of High Energy Physics* **2021**, 62 (2021).
- [27] Jae Dong Noh, “Operator growth in the transverse-field Ising spin chain with integrability-breaking longitudinal field,” *Phys. Rev. E* **104**, 034112 (2021).
- [28] Anatoly Dymarsky and Alexander Gorsky, “Quantum chaos as delocalization in Krylov space,” *Phys. Rev. B* **102**, 085137 (2020).
- [29] Pawel Caputa, Javier M. Magan, and Dimitrios Patramanis, “Geometry of Krylov Complexity,” [arXiv:2109.03824](https://arxiv.org/abs/2109.03824).
- [30] Anatoly Dymarsky and Michael Smolkin, “Krylov complexity in conformal field theory,” [arXiv:2104.09514](https://arxiv.org/abs/2104.09514).
- [31] Daniel J. Yates, Alexander G. Abanov, and Aditi Mitra, “Dynamics of almost strong edge modes in spin chains away from integrability,” *Phys. Rev. B* **102**, 195419 (2020).
- [32] Daniel J. Yates and Aditi Mitra, “Strong and almost strong modes of Floquet spin chains in Krylov subspaces,” *Phys. Rev. B* **104**, 195121 (2021).
- [33] Arijeet Pal and David A. Huse, “Many-body localization phase transition,” *Phys. Rev. B* **82**, 174411 (2010).
- [34] D.M. Basko, I.L. Aleiner, and B.L. Altshuler, “Metal-Insulator transition in a weakly interacting many-electron system with localized single-particle states,” *Ann. Phys.* **321**, 1126–1205 (2006).
- [35] Vadim Oganesyan and David A. Huse, “Localization of interacting fermions at high temperature,” *Phys. Rev. B* **75**, 155111 (2007).
- [36] Rahul Nandkishore and David A. Huse, “Many-body localization and thermalization in quantum statistical mechanics,” *Annu. Rev. Condens. Matter Phys.* **6**, 15–38 (2015).
- [37] Rong-Qiang He and Zhong-Yi Lu, “Characterizing many-body localization by out-of-Time-Ordered correlation,”

- Phys. Rev. B* **95**, 054201 (2017).
- [38] Yichen Huang, Yong-Liang Zhang, and Xie Chen, “Out-of-Time-Ordered Correlators in Many-Body Localized Systems,” *Ann. Phys.* **529**, 1600318–n/a (2017).
- [39] Xiao Chen, Tianci Zhou, David A. Huse, and Eduardo Fradkin, “Out-of-time-order correlations in many-body localized and thermal phases,” *Ann. Phys.* **529**, 1600332 (2017).
- [40] Kevin Slagle, Zhen Bi, Yi-Zhuang You, and Cenke Xu, “Out-of-time-order correlation in marginal many-body localized systems,” *Phys. Rev. B* **95**, 165136 (2017).
- [41] Brian Swingle and Debanjan Chowdhury, “Slow scrambling in disordered quantum systems,” *Phys. Rev. B* **95**, 060201 (2017).
- [42] Ruihua Fan, Pengfei Zhang, Huitao Shen, and Hui Zhai, “Out-of-time-order correlation for many-body localization,” *Sci. Bull.* **62**, 707–711 (2017).
- [43] Dong-Ling Deng, Xiaopeng Li, J. H. Pixley, Yang-Le Wu, and S. Das Sarma, “Logarithmic Entanglement Lightcone in Many-Body Localized Systems,” *Phys. Rev. B* **95**, 024202 (2017).
- [44] Xiangyu Cao, “A statistical mechanism for operator growth,” *J. Phys. Math. Theor.* **54**, 144001 (2021).
- [45] John Z. Imbrie, “Diagonalization and many-body localization for a disordered quantum spin chain,” *Phys. Rev. Lett.* **117**, 027201 (2016).
- [46] John Z. Imbrie, “On Many-Body Localization for Quantum Spin Chains,” *J. Stat. Phys.* **163**, 998–1048 (2016).
- [47] David A. Huse, Rahul Nandkishore, and Vadim Oganesyan, “Phenomenology of fully many-body-localized systems,” *Phys. Rev. B* **90**, 174202 (2014).
- [48] V. S. Viswanath and Gerhard Müller, *The Recursion Method: Applications to Many-Body Dynamics*, Lecture Notes in Physics Monographs (Springer-Verlag, Berlin Heidelberg, 1994).
- [49] Ilia Khait, Snir Gazit, Norman Y. Yao, and Assa Auerbach, “Spin transport of weakly disordered Heisenberg chain at infinite temperature,” *Phys. Rev. B* **93**, 224205 (2016).
- [50] Rahul Nandkishore, Sarang Gopalakrishnan, and David A. Huse, “Spectral features of a many-body localized system weakly coupled to a heat bath,” *Phys. Rev. B* **90**, 064203 (2014).
- [51] Sonika Johri, Rahul Nandkishore, and R. N. Bhatt, “Many-body localization in imperfectly isolated quantum systems,” *Phys. Rev. Lett.* **114**, 117401 (2015).
- [52] David Pekker, Bryan K. Clark, Vadim Oganesyan, and Gil Refael, “Fixed Points of Wegner-Wilson Flows and Many-Body Localization,” *Phys. Rev. Lett.* **119**, 075701 (2017).
- [53] Vipin Kerala Varma, Abhishek Raj, Sarang Gopalakrishnan, Vadim Oganesyan, and David Pekker, “Length scales in the many-body localized phase and their spectral signatures,” *Phys. Rev. B* **100**, 115136 (2019).
- [54] Sarang Gopalakrishnan and S. A. Parameswaran, “Dynamics and Transport at the Threshold of Many-Body Localization,” *Phys. Rep.* **862**, 1–62 (2020).
- [55] J. Herbrych, M. Mierzejewski, and P. Prelovšek, “Relaxation at different length-scales in models of many-body localization,” [arXiv:2110.15635](https://arxiv.org/abs/2110.15635).
- [56] Maksym Serbyn, Z. Papić, and Dmitry A. Abanin, “Local conservation laws and the structure of the many-body localized states,” *Phys. Rev. Lett.* **111**, 127201 (2013).
- [57] Anushya Chandran, Isaac H. Kim, Guifre Vidal, and Dmitry A. Abanin, “Constructing local integrals of motion in the many-body localized phase,” *Phys. Rev. B* **91**, 085425 (2015).
- [58] Fabian Ballar Trigueros, *Operator Growth and Krylov Complexity in Many-Body Localization*, Master’s thesis, University of Waterloo, Ontario, Canada (2021).